Deregulation of Exosomal miR-17, miR-20a and TGFBR2 in Head and Neck Cancer Patients

Muhammad Rizwan, PhD[1] (iD), Ishrat Mahjabeen, PhD[1] (iD),
Muhammad Shahbaz Haris, MS[1], Fouzia Qayyum, MBBS[2],
and Mahmood Akhtar Kayani, PhD[1] (iD)

Abstract

Introduction: Exosomes play significant roles in transferring cargo materials like proteins, RNAs (including miRNAs), and DNA. However, the role of serum exosome shuttled RNAs and miRNAs in head and neck cancer (HNC) remains unclear. This study assessed the diagnostic and prognostic significance of exosomal *miR-17*, *miR-20a*, and *TGFBR2* in HNC patients. **Methods:** Exosomes were isolated, from 400 confirmed HNC patients and 400 healthy controls, and characterized by NTA, TEM, Immunolabelling, and ELISA. Quantitative PCR was used to check the expressions of exosomal molecules. Oxidative stress was also measured through ELISA in cancer patients and healthy controls. **Results:** Data analysis revealed significant dysregulation in the expressional levels of miR-17 (p < .0001), miR-20a (p = .0003), and *TGFBR2* (p = .0005), which were found associated with aggressiveness and poor survival of HNC patients. Spearman correlation revealed a positive statistically significant association between miR-20a versus miR-17 (r = 0.534; p < .01), while a negative correlation was found between *TGFBR2* versus miR-17 (r = −0.240; p = .015). Significantly decreased levels of peroxidase (POD) (p < .0001) and an increased level of 8-Oxoguanine (p < .0001) were observed. **Conclusion:** The results showed that these exosomal miRNAs and target gene may serve as potential and noninvasive diagnostic and prognostic markers for head and neck cancer patients.

Keywords

exosome, head and neck cancer, miRNA-17-92 cluster, *miR-17*, *miR-20a*, *TGFBR2*, biomarker

Introduction

Head and neck cancer (HNC) is responsible for almost 6% of all cancers,[1] with over 830 000 new cases and over 430 000 deaths globally each year.[2] Alarmingly, the incidence of HNC is projected to rise by 30% annually by 2030.[3,4] HNC encompasses anatomical sites including the oral cavity, pharynx, hypopharynx, larynx, and nasal cavity. The oral cavity region includes buccal mucosa, lip, mouth floor, hard palate, anterior tongue, retromolar trigone, and upper/lower gingiva. The pharynx region consists of the nasopharynx, and oropharynx (tonsils area, soft palate, posterior pharyngeal wall, and tongue base.) The hypopharynx includes the bottom of the throat and pyriform sinuses. The larynx region consists of the glottic, subglottic, and supraglottic larynx. The nasal cavity and paranasal sinuses include ethmoid, maxillary, frontal sinuses, and sphenoid. HNC includes different histological subtypes while squamous cell carcinoma (SCC) is the most prevalent form, constituting 90% of cases.[3] The traditional tissue biopsy

method for HNC cannot track disease progression or may increase tumor metastasis potential due to misleading results based on differences in cell morphology, and leads towards poor survival and prognosis.[5] Despite advances in treatment, patients with advanced-stage HNC show a 5-year survival rate of less than 60% with poor prognosis,[6] suggesting the need for new biomarkers to improve prognosis and treatment outcomes. Liquid biopsy which is a minimal invasive approach using biofluids of blood and urine samples, holds potential to

[1] Cancer Genetics & Epigenetics Research Group, Department of Biosciences, COMSATS University Islamabad, Islamabad, Pakistan
[2] Department of ENT, Bahawalpur Victoria Hospital, Bahawalpur, Pakistan

Corresponding Author:
Ishrat Mahjabeen, Dr., Cancer Genetics & Epigenetics Research Group, Department of Biosciences, COMSATS University Islamabad, Park Road Islamabad, Pakistan.
Email: ishrat.mahjabeen@comsats.edu.pk

diagnose and real time-monitoring of cancer.[7] These biofluids contained some biological carriers whose secretion rate changed due to disease initiation and pathogenesis. Exosomes are important for properly tracking disease progression among these biological carriers.

Exosomes are a subclass of extracellular vesicles with a size range of 40-160 nm. These vesicles are secreted by both normal and cancerous cells.[8] Exosomes play roles in transfer of cargo materials like proteins, DNA, mRNA, and microRNAs (miRNAs) from donor cells to recipient cells, thus playing a role in intercellular communication.[9] Exosomes may also play a role in the deregulation of different pathways or change in the cellular fate of neighboring cells through exosomal content (specifically miRNAs) released by specific cells. This showed a possible role of exosomes in the progression, initiation, or drug resistance of cancer cells.[10] Exosomal miRNAs have been linked with phenotypes of several cancers in different studies[11,12] indicating their potential as diagnostic biomarkers in HNC.[13]

MicroRNAs (miRNAs) play crucial roles in the development of different cancers. This includes the dysregulation of the miRNA-17-92 cluster, which has been studied in different cancers.[11,12] The two important members of the miR-17-92 cluster, miR-20 and miR-17-5p, are also called the miR-17 family based on sequence composition.[14] Deregulation of miR-17 has been reported in HNC[15] and miR-20 in HPV-positive oropharyngeal carcinoma of HNC.[16] Both miRNAs of the miR-17 family have equivalent functions by controlling the same target genes as their same seed sequences.[17] It has been reported that miR-20a and miR-17 directly target *TGFBR2* and regulate the TGF-signaling pathway[18] that controls several cellular processes including cell cycle arrest, epithelial to mesenchymal transition, apoptosis, and migration.[18] The study has reported the expression deregulation of *TGFBR2* resulted in an aggressive type of HNC.[19] Deregulated expressions of miRNAs have been studied and reported in HNC patients. Still, fewer studies are available on the role of these exosomal miRNAs in HNC. In this study, miR-17-92 cluster microRNAs (miR-20a and miR-17) and target gene *TGFBR2* were selected for analysis. Expressions of miR-20a, miR-17, and *TGFBR2* were analyzed in serum exosomes of HNC patients and compared with healthy controls. The expression results were also correlated with the clinical parameters to elucidate the potential of exosomal miRNAs as diagnostic and prognostic biomarkers for HNC patients.

Methods

Samples Collection and Clinical Data

The samples of HNC patients and healthy individuals (taken as controls) were collected over 2 years from May 2021 to June 2023 from collaborating hospitals. The current study was authorized by the institutional ethical review committee of the university and the collaborating hospitals. GPower sample size calculator (GPower 3, The university of Dusseldorf, Dusseldorf, Germany) software was utilized to calculate the sample size; α was set to 0.05, and 1-β to 0.90. The current research included 400 verified HNC and 400 age- and gender-matched healthy individuals as control

samples as shown in Supplementary Table S1. Samples were taken only after informed consent from all participants.

Demographic parameters along with clinical records were collected from patients questionnaires and histopathological reports. In present study cohort, AJCC staging was followed to assess the TNM staging and further categorized into early and advanced stages. Tumor stages (T-stage) were divided into early T-stages (T1 and T2) versus advanced T-stages (T3 and T4). Lymph node stages (N-stage) were compared between early N-stages (N0) and advanced N-stages (N1-N3), while metastasis stages were divided into no-metastasis (M0) versus metastasis-stage (M1). In the case of clinical stages, patients were also divided into two stages including early clinical stages (C1-C2) and advanced clinical stages (C3-C4), as shown in Supplementary Table S1. The smoking status of HNC patients was categorized based on self-reported history and mentioned in Supplementary Table S1. The participants were asked about their smoking history, current smoking status, and the number of packs per day. This study has included three types of tobacco use which are paan, naswar and cigarets. As intake of these agents varies from individuals to individuals, a broad definition of smoking was introduced here. Alcohol use is another significant risk factor for HNC but most of the participants were not drinking or were unwilling to respond to this question.

Furthermore, the patients were categorized based on their treatment status at the time of sample collection. The patients who were treated with any form of therapeutic strategy including surgery, radiation, or chemotherapy, were classified as treated patients. Patients who were newly diagnosed and had not yet been treated with any form of therapeutic strategy were classified as untreated patients. The data on the treatment status of HNC patients is mentioned in Supplementary Table S1.

The control and patient samples with other diseases, such as hypertension, diabetes, familial diseases, or suffering from conditions other than HNC, were excluded. For serum extractions, 2 ml of blood was taken from patients and healthy controls. Blood samples were spun at 3000 and 10 000 × g for 15 and 20 min at 4 °C, followed by serum storage at −80 °C.

After collecting samples, we follow up with the patients for 5 years (starting from the time of diagnosis). Half of the patients died during the follow-up duration with no report of recurrence. So far 192 patients have died, and the remaining 208 patients have been in good health according to follow-up results.

Exosome Purification

For exosome purification, a total exosome isolation kit (provided by Invitrogen, USA) and ultracentrifugation methods were used for exosomes extraction from HNC serum samples and controls as described previously.[20] The first step was use of a total exosome isolation kit, following the guidelines supplied by the manufacturer. In brief, the frozen serum samples were thawed in a water bath set at a temperature of 25 °C. After this step, samples were centrifuged for 30 min at 2000 × g to enhance the purification process by removing the cellular debris and then subjected to RNase-free tube. The 500 µl

clarified serum was mixed with 100 μl of exosome extraction reagent and this serum/reagent mixture was gently vortexed and then incubated for 30 min. Next, the specimens underwent centrifugation at 10 000 × g for 10 min, following the supernatant was removed. Then the pellet was dissolved in PBS and the second step exosome pellet was purified by transferring it into 1.5 mL polyallomer ultracentrifugation tubes (Beckman Coulter, Fullerton, CA). Then the samples were ultracentrifuged at 110 000 × g (Beckman Coulter Opima Max) for 1 h at 4 °C. Exosome pellets were washed with PBS and the ultracentrifugation step was repeated. The pellets of exosomes were then resuspended in 100 μl of 1 × PBS and stored at −80 °C for further downstream analysis.

Transmission Electron Microscopy (TEM)

The exosome pellets were diluted at a ratio of 1:10 ratio in PBS and the morphology of exosomes was captured through a transmission electron microscope (TEM) as described previously.[20] 5 μl of exosome sample was applied on carbon-coated grids (EMS www.emsdiasum.com) which was hydrophilic through the application of 30 s glow discharge (25 mA). Extra liquid was wiped away through Whatman 1 filter paper followed by briefly floated in water to remove salt or phosphate, blotted once more with filter paper, and stained for 20-30 s with 0.75% uranyl formate (EMS catalog 22451). Extra stains were wiped with filter paper and grids were observed in JEOL 1200 EX TEM.

Immunogold Labeling

Exosome confirmation was performed through immunoelectron microscopy.[20] 5 μl of exosome sample was loaded on the carbon-coated grid. Exosome blocking was performed through 1% BSA for 10 min and then immunolabelled with primary antibody, anti-human CD63 (BD Pharmingen 556019) for 30 min. The sample was washed in PBS for 10 min, followed by gold-labeled secondary antibody (Abcam ab6709) for 20 min. The sample was washed in PBS and then in water for 5 and 10 min respectively. Whatman #1 filter paper was used to remove excess liquid and then samples were subjected to staining with 0.75% uranyl formate for 15 s. Excess liquid was removed with filter paper and grids were observed in JEOL 1200 EX transmission electron microscope.

Nanosight Nanoparticle Tracking Analysis (NTA)

Nanosight LM10 system (Nanosight Ltd) was used to calculate the mean size and concentration of isolated exosomes.[20] The exosome samples were diluted at 1:70 in sterile-filtered PBS. Exosomes were illuminated through a blue laser (405 nm) and their Brownian movement was recorded for 60 s. The size distribution and nanoparticle concentration were calculated using Nanosight particle tracking software. During analysis, all settings were kept the same and a minimum of three measurements were taken for each sample to calculate the representative measurement.

ELISA

The identification and quantification of exosomes were performed utilizing ExoELISA-Ultra complete kits (System Biosciences, Inc.) which enable the detection of the exosomal protein markers including *CD9*, *CD63,* and *CD81*. ELISA was performed according to manufacturer instructions as described previously.[20] Briefly, exosome samples were diluted using a coating buffer and prepared as per the manufacturer's instructions. Then 50 μl of protein buffer and exosome specimens were added in microtiter wells and incubated at 37 °C for an hour after covering the wells. The wells were emptied by inverting followed by three times washing with 100-200 μl 1 × wash buffer. Next, 50 μl of *CD9*, *CD63,* and *CD81* diluted primary antibodies were introduced to each well followed by 60 min of incubation at 37 °C and then the plate was further washed three times with 1 × wash buffer. Then, 50 μl of diluted secondary antibody (1:5000 in blocking buffer) was poured into each well. The plate was again incubated for 60 min and rewashed. The assay was then ceased by adding 50 μl of colorimetric substrate (super sensitive TMB ELISA) and 50 μl of stop buffer. The protein samples were then quantitated using a microplate reader (AMP Platos R II), following optical density (OD) at 450 nm. The resulting values were plotted against the standard curve provided by the kit. The samples were analyzed in triplicates and for each concentration (pg/ml), results were reported as mean ± SD.

RNA Isolation from Serum Exosomes

Exosome pellets were mixed with TRIzol reagent (Invitrogen, CA, US) treatment according to manufacturer's guidelines in order to extract total RNA.[20] In short, a volume of 1 milliliter of TRIzol reagent was combined with 200 μl of chloroform and poured into the samples. Following centrifugation at 12 000 × g at 4 °C for a duration of 15 min, the resulting supernatant from each sample was added in separate eppendorf and mixed with 500 μl of isopropanol for a duration of 10 min at −20 °C. This step was repeated with centrifugation at 12 000 × g at 4 °C for 10 min and then supernatants were discarded. Subsequently, RNA pellets underwent washing process utilizing 75% ethanol, followed by resuspension in 10 μl of nuclease-free water. After RNA isolation, the concentration and purity of isolated RNA were evaluated through a nanodrop spectrophotometer (Thermo Scientific) through measuring OD at 260/280 nm. Subsequently, RNA samples were stored at −80 °C for further utilization.

cDNA Synthesis and Expression Analysis

The RevertAid first-strand cDNA synthesis kit (Thermo Scientific) was used to prepare the reverse transcript mixture for complementary DNA (cDNA) following the instructions

provided by the manufacturer. Primers of *miR-17*, *miR-20a*, *U6*, *TGFBR2*, and *β-actin* were synthesized using PrimerQuest Tool (Integrated DNA Technology, IA, USA). Detailed primer sequences with optimized annealing temperatures are listed in Supplementary Table S2. The 10 µl reaction mixture for each molecule was prepared with 1 µl of cDNA of each sample along with each forward and reverse primer, 4 µl of dye (2x Sybr Green, Invitrogen), and afterward 4 µl of PCR water. Step-one-plus real-time PCR instrument (Applied Biosystems, MA, US) was used for quantitative PCR of related gene and selected miRNAs. The PCR reaction was carried out using 96 well plates and initial denaturation at 95 °C for 6 min, then 40 cycles of 95 °C for 30 s, and at the final step of annealing temperature for 30 s. The resulting data was analyzed with the $2^{-\Delta\Delta Ct}$ method relative to reference β-actin for gene and U6 for miRNAs as reported by Livek and Schmittgen.[21]

Oxidative Stress Measurement

Oxidative stress levels in isolated exosomes of HNC patients compared to controls were evaluated using the ELISA as reported by Hussain et al.[22] Oxidative stress was assessed by (i) analyzing the levels of antioxidant enzyme *Peroxidase* level (*POD*) and by (ii) measuring the ROS, *8-Oxoguanine* (*8-OHdG*) in isolated exosomes of HNC patients and controls. *Peroxidase* level (*POD*) was measured using the peroxidase ELISA kit (Abcam, USA). The 8-Oxoguanine (8-OHG) level was measured using the available ELISA kit of 8-hydroxy 2 deoxyguanosine (Abcam, USA). The concentrations of antioxidant and reactive oxygen species (ROS) levels were then quantitated by a microplate reader (AMP Platos R II) at OD 450 nm. The resulting values were then plotted against a standard curve. The samples were analyzed in triplicates and reported as mean ± SD for each concentration (pg/ml).

Statistical Analysis

The statistical tests used in the current study are one-way ANOVA and the student t-test assessed significance between groups. Spearman correlation was utilized for clinical correlations. ROC curve and area under the curve (AUC) were used to check the diagnostic ability and accuracy of chosen miRNAs and genes by measuring sensitivity and specificity. Furthermore, Kaplan Meier and Cox regressions were used to check the prognostic significance of selected molecules in HNC patients. Statistical analysis was performed using SPSS (IBM SPSS, version 26) and GraphPad Prism (version 8.0.2, US). p < .05 was taken as statistically significant.

Results

Demographic and Clinical Parameters of the Study Cohort

The study cohort consisted of 400 HNC patients and 400 age and gender-matched healthy controls were used in the present study. The demographic and clinical parameters of the current study cohort included age, gender, anatomical site of cancer (pharynx, oral cavity, and larynx), smoking status, grades of cancer (poorly, moderately, and well-differentiated), T-staging (T1-T4), N-staging (N0-N3), metastatic stages (M0 and M1) and treated versus untreated HNC patients as shown in Supplementary Table S1.

Serum Exosome Characterizations

Exosomes were isolated from serum samples obtained from HNC patients and control samples. The characterization of isolated exosomes was carried out using various techniques including NTA, TEM, TEM-Immunolabelling, and ELISA. The results are shown in Figure 1. TEM was used to characterize morphology and negative staining of purified exosomes revealed a spherical shape with anticipated exosome size range (30-150 nm) with membrane integrity (Figure 1A). Immunogold labeling was used to confirm the protein surface marker specific to CD63, a marker for the identification of exosomes. Positive immunolabelling was observed using Transmission Electron Microscope and the results are shown in Figure 1B. NTA was used for the size distribution of exosomes and the number of particles per µL. Brownian movement of exosomes was recorded, and measurements showed the model size of 100 nm, confirming particle populations within exosome size range (Figure 1C). The positive confirmation of isolated exosomes was obtained through ELISA using exosome-specific protein markers including *CD9*, *CD63*, and *CD81*. The results are shown in Figure 1D.

Relative Expression of Exosomal miR-17 in HNC

The expression level of exosomal miR-17 was analyzed and compared in HNC patients and controls. Significantly reduced expression of miR-17 (average value 0.12 ± 0.5) was found in HNC patients (p < .0001) versus control samples (Figure 2A). This miR-17 expression was analyzed statistically in different demographic and histological categories of HNC patients.

When analyzed a significant downregulation was observed in patients with <52 years mean age (p = .024) and smoker patients (p = .0154). In the case of smoking status in controls, a significantly increased level of miR-17 (p = .0444) was observed in smoker controls compared to nonsmoker controls, as shown in Supplementary Figure 1A. In histopathological parameters, significant downregulation was observed in laryngeal cancer (p = .0429), poorly differentiated cancers (p = .0264), advanced T-staging (p = .0157), advanced N-stages (p = .0013), M1-stage (p = .0185) and aggressive clinical stage (p = .0094). These results are shown in Figure 2B.

Patients were also divided into treated versus untreated and when analyzed non-significant decreased expression was assessed in untreated patients (p = .3610) (Figure 2C). Figure 2C also shows that significant downregulation was assessed in under-treatment patients (p < .0001) and untreated patients (p < .0001) when compared with respective controls.
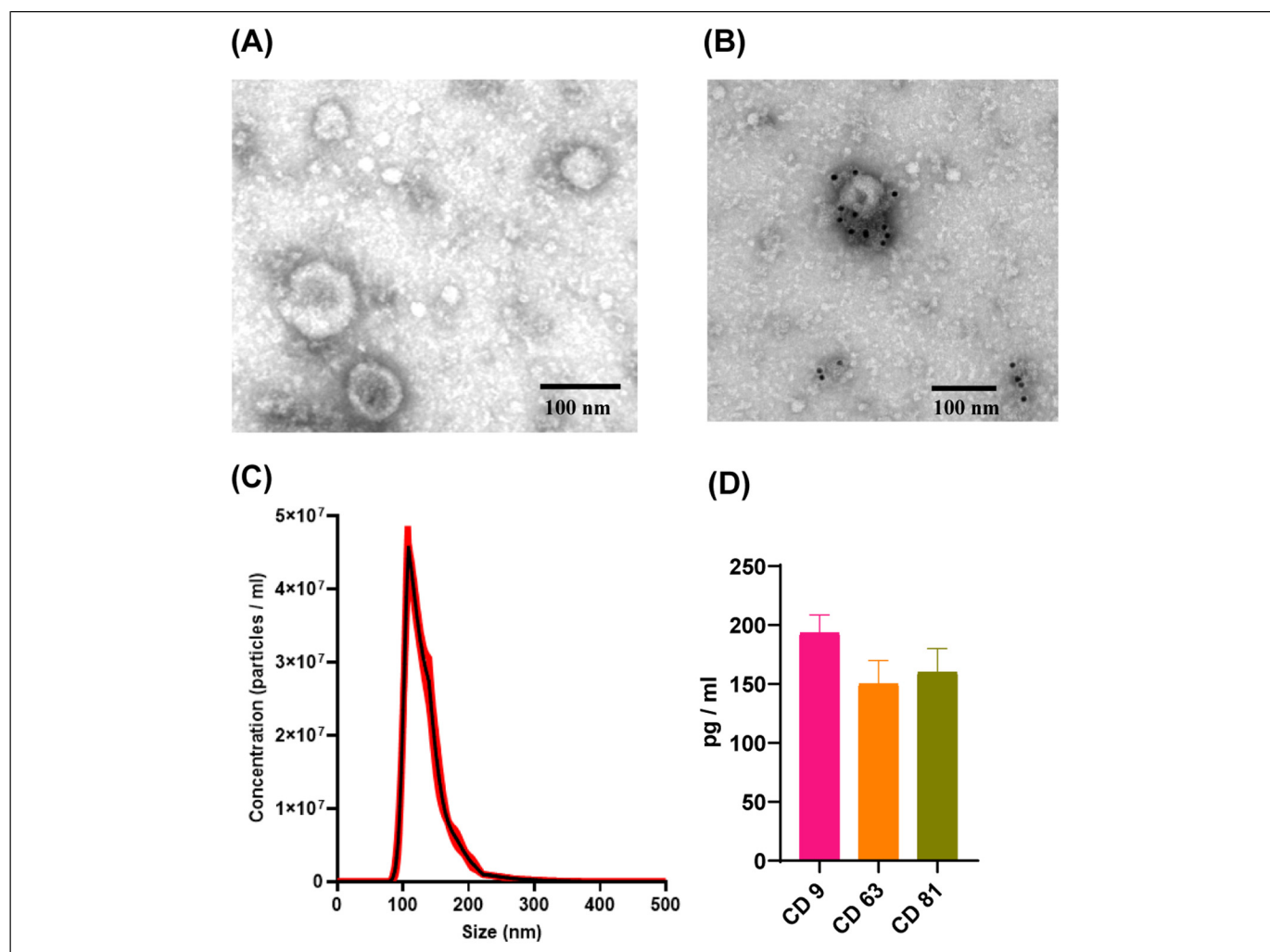
Figure 1. Exosomes characterizations (A) TEM negative staining of exosomes revealed sphere shaped morphology of serum exosomes (scale bar = 100 nm). TEM micrograph showed exosomes size with an acceptable size range. (B) CD63 immunogoldlabelling of exosomes and imaged through TEM. (C) Size distribution and concentration of exosomes analyzed with NTA of combining serum samples. (D) ELISA-based detection of serum exosomal protein surface markers CD9, CD63 and CD81. For each concentration (pg/ml) of three proteins, the results are shown as mean ± SD.

Relative Expression of Exosomal miR-20a in HNC

Exosomal miR-20a was found to be significantly downregulated in HNC patients versus controls (p = .0003) (Figure 3A). Significant downregulated expression of miR-20a (average value 0.60 ± 0.45) was observed in HNC patients for gender (female vs male) (p = .0448), and smoker patients (p = .0209), as shown in Figure 3A. In the case of smoking status in controls, a nonsignificant difference in miR-20a level (p = .3152) was observed in smoker controls compared to nonsmoker controls, as shown in Supplementary Figure 1B. In clinical characteristics of the study, exosomal *miR-20a* was significantly downregulated in the oral cavity subtype of HNC (p = .0002), poorly differentiated cancers (p = .0156), advanced T-stages (p = .0046), advanced N-stages (p = .0191), metastatic-phase (M1) (p = .0093) and aggressive clinical phases (p = .0104) (Figure 3B). Non-significant downregulation was observed in untreated

versus treated HNC patients (p = .0689) and under-treatment patients versus controls (p = .1318) (Figure 3C). At the same time, significant downregulation was observed in untreated patients versus controls (p = .0373) (Figure 3C).

Relative Expression of Exosomal TGFBR2 in HNC

Exosomal *TGFBR2* was found significantly upregulated in patients of HNC when compared with controls (p = .0005) (Figure 4A). *TGFBR2* was significantly upregulated in smoker patients (p = .0025) (Figure 4A). In the case of smoking status in controls, a nonsignificant difference in *TGFBR2* level (p = .4150) was observed in smoker controls compared to nonsmoker controls, as shown in Supplementary Figure 1C. *TGFBR2* was also observed upregulated in poorly differentiated grades (p = .0199) and advanced clinical stages
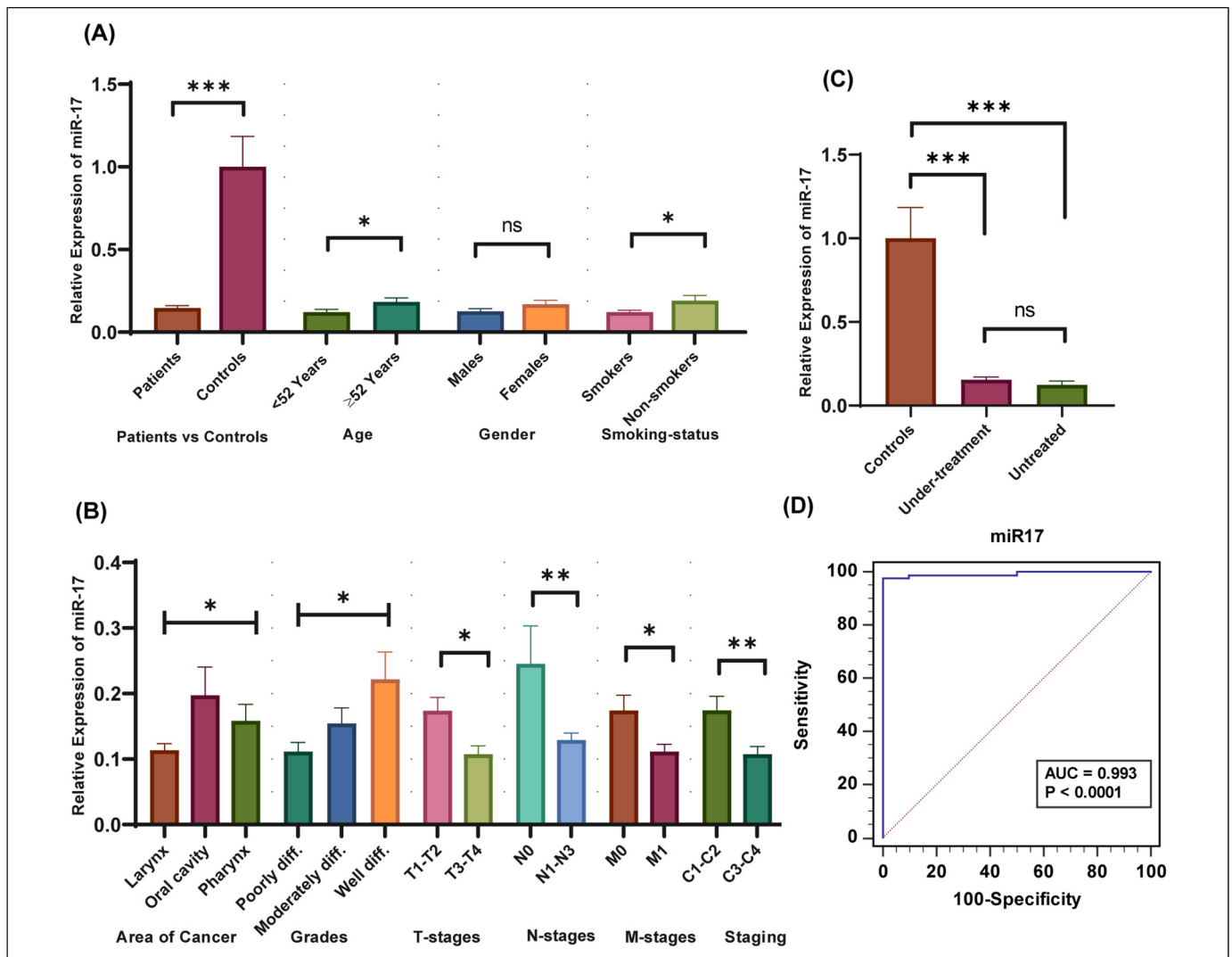
Figure 2. Expression analysis of miR-17 in exosomes of HNC patients and controls. (A) Expression levels of miR-17 in HNC patients versus controls and in demographic parameters. (B) miR-17 expression analysis in clinicopathological parameters of HNC. (C) miR-17 expression levels in HNC treated versus un-treated versus controls. (D) AUC-ROC analysis of miR-17 in HNC patients.

(p = .0128) compared to early clinical stages HNC patients (Figure 4B). Significant upregulation of *TGFBR2* was observed in advanced T-stage (p = .0130), advanced N-stage (p = .0107), and metastatic stage (M1, p = .0092) (Figure 4B). Moreover, significant upregulation of *TGFBR2* was found in under-treatment (p = .0002) and untreated HNC patients versus controls (p = .0031) as shown in Figure 4C.

Correlation Between Exosomal miR-17, miR-20, TGFBR2, Demographic and Clinicopathological Parameters

Spearman correlation was used to analyze gene-gene, gene-parameter, and parameter-parameter interactions. These results are shown in Table 1. In the current study, a significant negative correlation was observed between smoking and gender (r = −0.442; p < .01), smoking, and types of HNC (r = −0.209; p = .036). Table 1

shows a significant positive correlation between N-stages and T-stages (r = 0.345; p < .01), M-stages and T-stages (r = 0.294; p = .003), M-stages and N-stages (r = 0.283; p = .004). A significant negative correlation was observed in cases of gene-parameter including miR-20a and smoking (r = −0.241; p = .015), *TGFBR2*, and M-stages (r = −0.216; p = .030). In gene-gene correlation, a positive significant correlation was identified between miR-20a and miR-17 (r = 0.534; p < .01). However, a negative correlation was observed between *TGFBR2* and miR-17 (r = −0.240; p = .015).

ROC Curve Analysis of Exosomal miR-17, miR20a, and TGFBR2

ROC curve analysis was performed for exosomal miR-17, miR-20a, and *TGFBR2*. The results of ROC curve analysis are presented in Figures 2 to 4. The area under the curve (AUC)
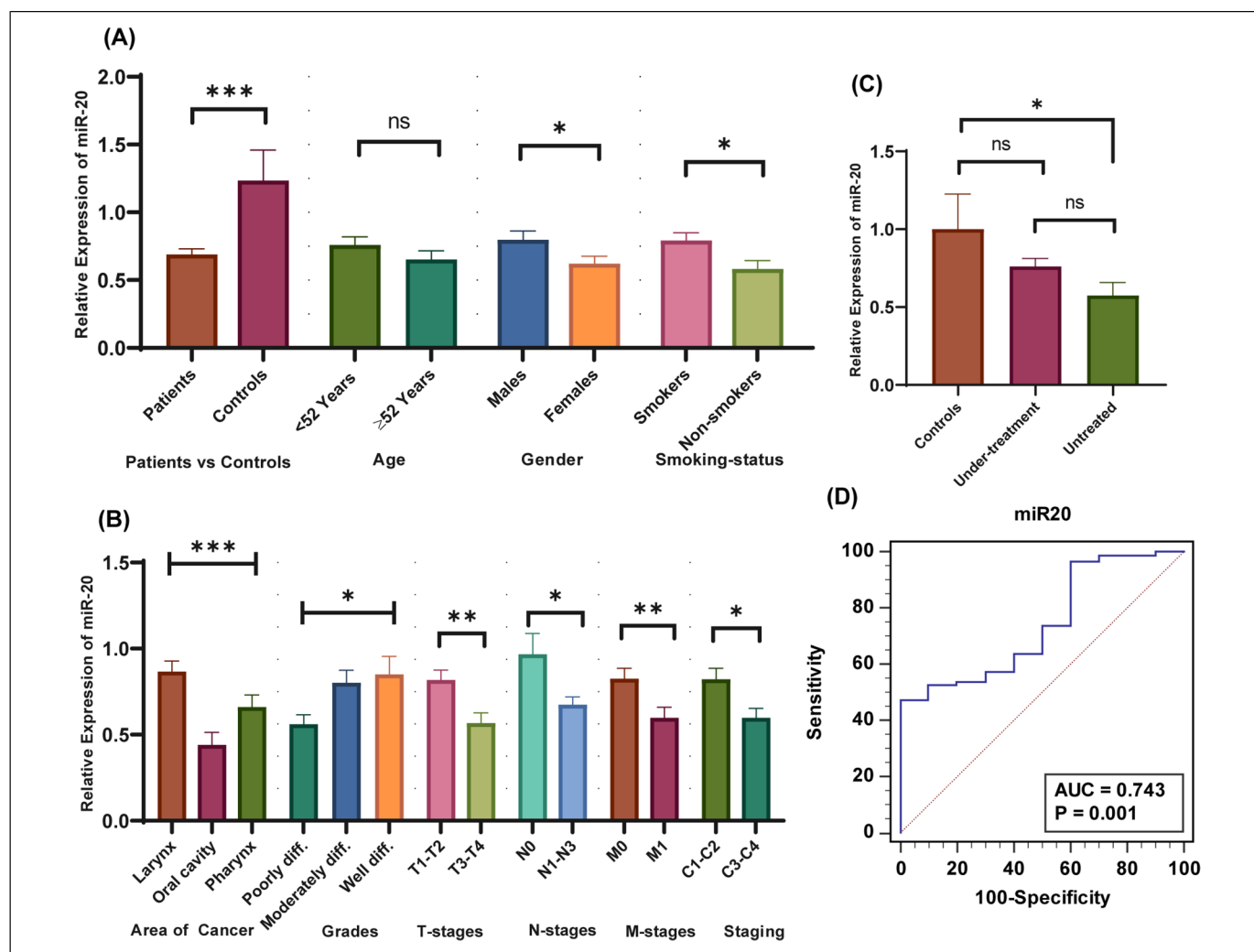
Figure 3. Expression analysis of miR-20a in exosomes of HNC patients and controls. (A) miR-20a expression levels in HNC patient's versus controls and in HNC demographic parameters. (B) miR-20a expressions in clinical parameters of HNC. (C) miR-17 expression levels in HNC treated versus un-treated versus controls. (D) AUC-ROC analysis of miR-20a in HNC patients.

for miR-17 was found 0.993 with 97.80% sensitivity and 100% specificity (95%CI: 0.952-1.000; p < .0001) in HNC patients (Figure 2D). miR-20a showed 0.743 AUC (sensitivity: 47.25; specificity: 100; 95%CI: 0.646-0.825; p = .0013) (Figure 3D). The AUC for *TGFBR2* was 0.831 (sensitivity: 0.33; specificity: 100; 95%CI: 0.743-0.898; p < .0001) (Figure 4D).

Kaplan Meier Analysis

Deregulated expression of selected exosomal miRNAs was correlated with the survival rate of patients, using Kaplan Meier analysis. The results are shown in Figure 5. In Kaplan Meier analysis expression levels of microRNAs and related gene were classified into downregulation and upregulation based on expression optimal cutoff values. These optimal cutoff values were determined using the X-tile program. The downregulation of exosomal microRNAs, miR-17 (p = .0318), and miR-20a (p = .0144) correlated with significantly reduced

survival of patients (Figure 5A and B). However, increased expression of *TGFBR2* gene (p = .0056) was found associated with significantly reduced survival (Figure 5C).

Cox Regression Analysis of Selected Molecules in HNC Patients

Univariate and multivariate Cox regression was used to confirm the results of Kaplan Meier analysis. The results are given in Table 2. Univariate Cox regression analysis revealed that dysregulation of miR-17 (HR = 1.64; p = .01), miR-20a (HR = 1.74; p = .01), and *TGFBR2* (HR = 2.86; p = .005) was correlated with overall decreased survival of patients (Table 2). The analysis also showed that clinical stage (HR = 2.32; p = .003), T-stage (HR = 2.17, p = .01), N-stage (HR = 2.66; p = .007), M-stage (HR = 4.11; p = .0001) and advance grade (HR = 2.21; p = .004) was associated with overall reduced patient survival (Table 2).
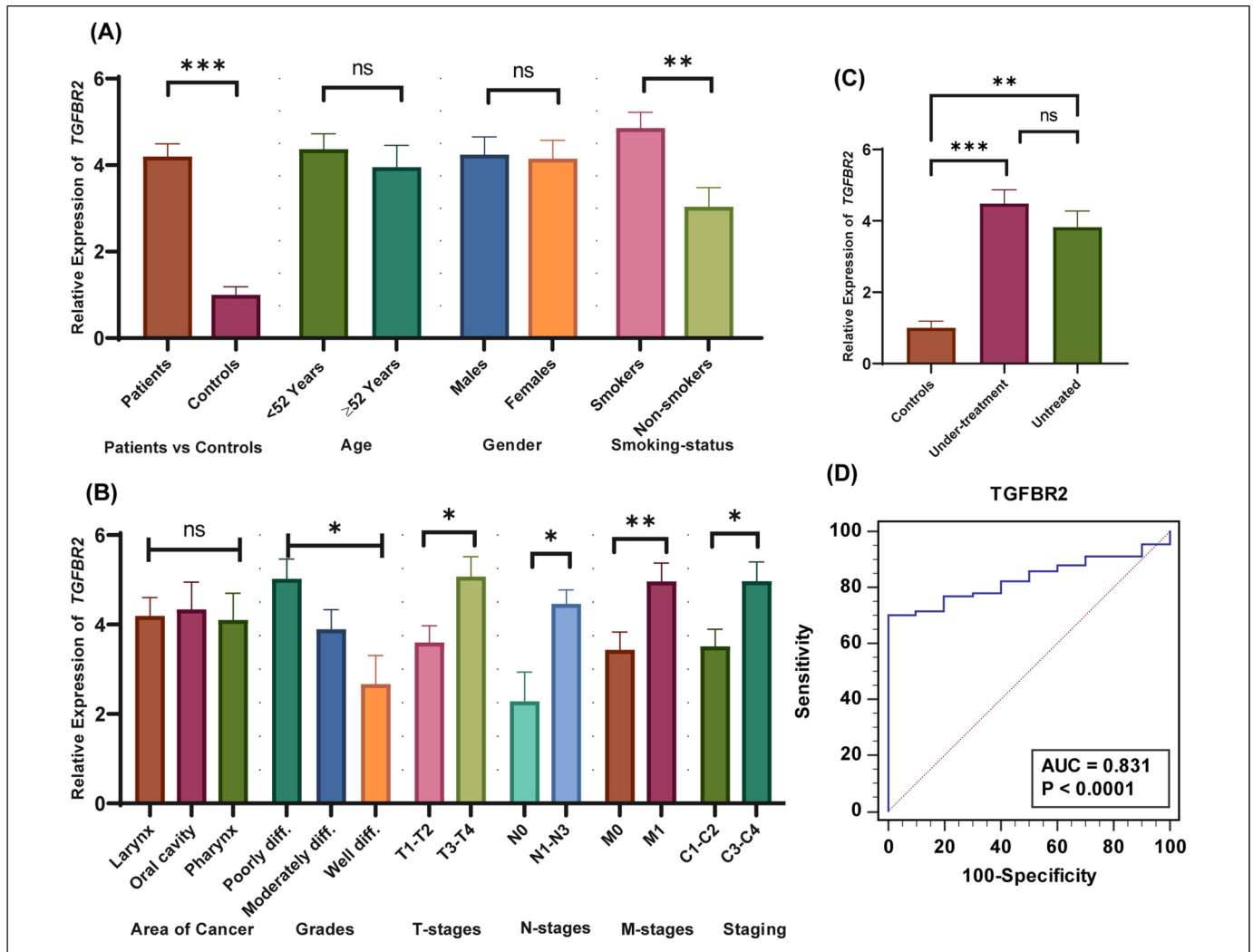
Figure 4. Expression analysis of *TGFBR2* in exosomes of HNC patients and controls. (A) Expression Analysis of *TGFBR2* in exosomes of HNC patient's versus controls and in HNC demographic parameters. (B) *TGFBR2* expressions in clinical parameters of HNC. (C) *TGFBR2* expressional results in HNC treated versus un-treated versus healthy controls. (D) AUC-ROC analysis of *TGFBR2* in HNC patients.

Table 1. Spearman Correlation Between Exosomal miR-17, miR-20, TGFBR2, Demographic and Clinical Parameters of HNC Patients.

	Gender	Age	Cancer area	Grade	Smoking	T-stage	N-stage	M-stage	miR-17	miR-20	*TGFBR2*
Gender	1.000	0.187	0.080	0.003	−0.442**	0.044	0.108	−0.011	−0.096	0.054	0.034
Age		1.000	−0.033	−0.009	−0.185	−0.051	−0.084	−0.049	0.149	0.074	−0.049
Type			1.000	0.094	−0.209*	0.055	−0.116	0.043	−0.009	0.180	0.112
Grade				1.000	−0.001	−0.137	0.012	−0.033	−0.030	0.043	0.019
Smoking					1.000	−0.076	−0.024	0.012	−0.045	−0.241*	−0.116
T-stage						1.000	0.345**	0.294**	−0.084	−0.120	−0.003
N-stage							1.000	0.283**	−0.034	−0.163	−0.050
M-stage								1.000	0.018	0.014	−0.216*
miR-17									1.000	0.534**	−0.240*
miR-20										1.000	−0.103
TGFBR2											1.000

** Correlation is significant at the 0.01 level (2-tailed).
* Correlation is significant at the 0.05 level (2-tailed).
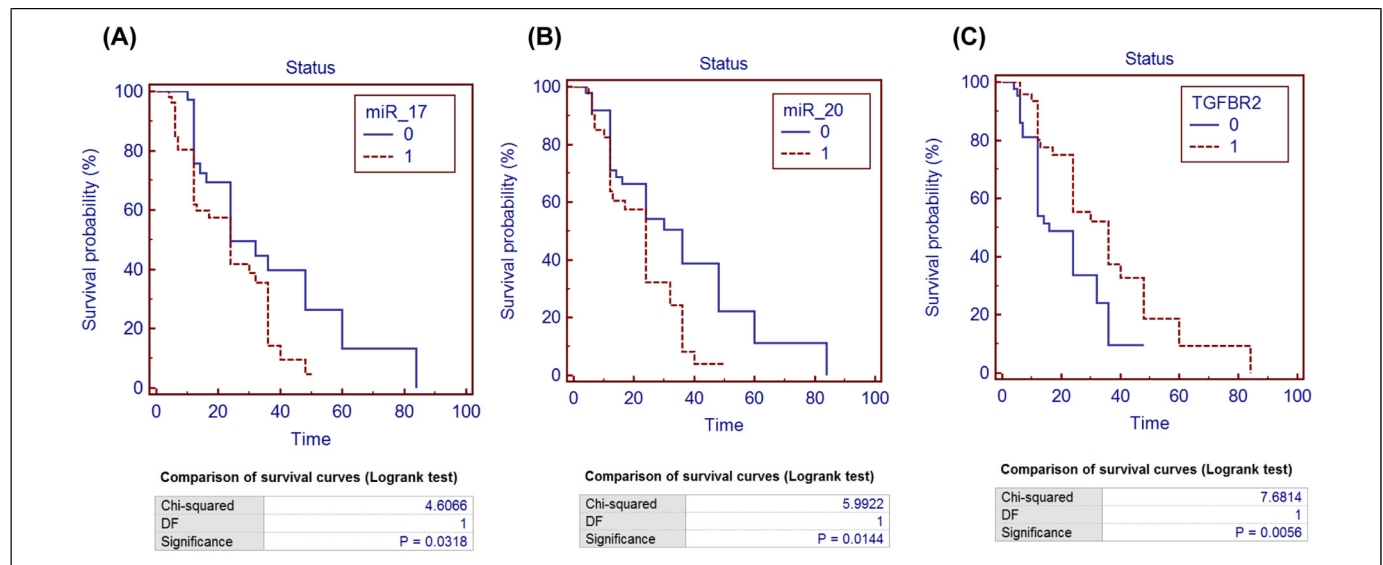
Figure 5. Survival analysis (A) Kaplan Meier analysis of miR-17 in serum exosome of HNC patients. (B) Kaplan Meier analysis of miR-20a in serum exosome of HNC patients. (C) Kaplan Meier analysis of *TGFBR2* in serum exosome of HNC patients. 0 show upregulation and 1 show the downregulation of selected microRNAs and gene in serum exosome of HNC patients. DF is degree of freedom.

Table 2. Univariant and Multivariant cox Regression Analysis of Exosomal miRNAs in HNC Patients.

Univariate analysis				Multivariate analysis			
Parameter	Hazard Ratio	95% CI	p-value	Parameter	Hazard Ratio	95% CI	p-value
miR-17	1.64	1.04-2.56	.01	miR-17	5.62	2.35-13.1	.0001
miR-20	1.74	1.14-2.65	.01	miR-20	4.91	2.20-10.95	.0001
TGFBR2	2.86	1.37-5.95	.005	*TGFBR2*	5.87	2.40-14.31	.0001
Age	0.23	0.02-2.07	.19	Clinical stages	3.29	1.49-7.22	.003
Gender	0.49	0.16-1.49	.628	T-stage	3.61	1.68-7.75	.001
Cancer area	1.04	0.82-1.31	.74	N-stage	2.98	1.39-6.38	.005
Smoking	0.99	0.94-1.04	.71	M-stage	3.91	1.74-8.81	.001
Clinical stages	2.32	1.33-4.04	.003	Grade	4.36	2.07-9.15	.0001
T-stage	2.17	1.20-3.91	.01				
N-stage	2.66	1.30-5.41	.007				
M-stage	4.11	2.01-8.37	.0001				
Grade	2.21	1.28-3.97	.004				

Multivariate Cox regression analysis suggested that deregulation of exosomal microRNAs miR-17 (HR = 5.62; p = .0001), miR-20a (HR = 4.91; p = .0001), and *TGFBR2* (HR = 5.87; p = .0001) was correlated with overall reduced patient survival (Table 2). The analysis also showed that the clinical stage (HR = 3.29; p = .003), T-stage (HR = 3.61; p = .001), N-stage (HR = 2.98; p = .005), M stage (HR = 3.91; p = .001), and grade (HR = 4.36; p = .0001) were found as independent prognostic parameters in HNC patients.

Oxidative Stress Evaluation in Exosomes of HNC Patients

Oxidative stress was evaluated in exosomes of HNC patients versus controls by measuring *Peroxidase* level (*POD*) and *8-Oxoguanine* (*8-OHdG*) levels. The results are shown in

Figure 6. Figure 6A revealed, a significantly decreased level of peroxidase level (*POD*) in exosomes of HNC (p < .0001) patients compared to controls. POD levels were associated with the clinical characteristics of HNC patients. Figure 6B shows the significantly decreased levels of POD in advanced clinical stages (p < .0013), late T-stages (p < .0023), advanced N-stages (p < .0003), metastatic stage (p < .0006) and in poorly differentiated grades (p < .0004). POD also showed significantly decreased levels in treated patients (p = .0007) versus untreated HNC patients. Figure 6C shows the significantly decreased level of POD in patients of different age groups (<52 years vs ≥52 years; p < .01) and smoking status (smokers vs nonsmokers; p < .01). Non-significant decrease in POD level was observed in the case of gender (males vs females; p = .16), as shown in Figure 6C.
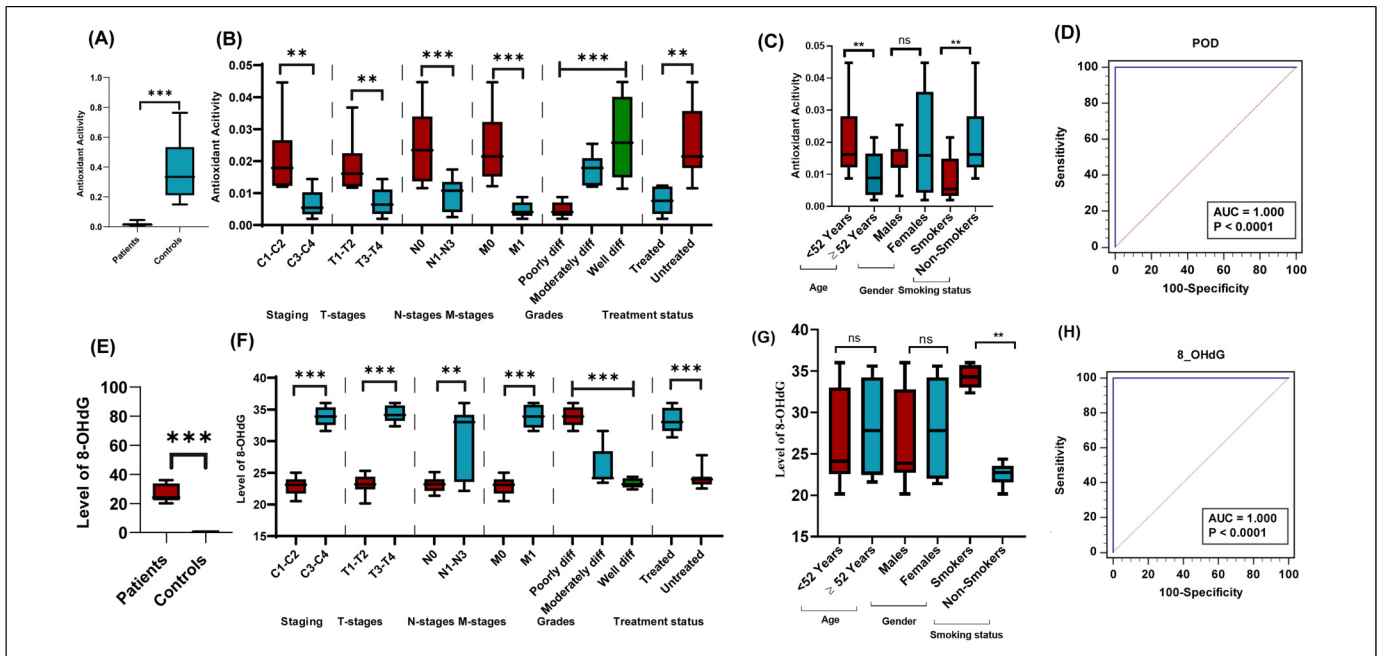
Figure 6. Measurement of oxidative stress in exosome of HNC patients (A) level of antioxidant enzyme, *peroxidase* (*POD*) in exosome of HNC patients compared to controls. (B) Association of POD levels with clinical characteristics of HNC patients. (C) ROC curve analysis of *POD* in exosome of HNC patients compared to controls. (D) *8-Oxoguanine* (*8-OHdG*) levels in exosome of HNC patients compared to controls. (E) Association of 8-OHdG levels with clinical characteristics of HNC patients. (F) ROC curve analysis of 8-OHdG in exosome of HNC patients.

In the case of *8-Oxoguanine* level, a significantly increased level was observed in exosomes of HNC patients (p < .0001) versus controls (Figure 6E). In association with clinical parameters, 8-OHdG showed significantly increased levels in advanced clinical stages (p < .0001), advanced T-stages (p < .0001), advanced N-stages (p = .0012), metastatic stage (p < .0001) and in poorly differentiated grades (p < .0001) (Figure 6F). The HNC treated patients showed significantly increased 8-OHdG levels (p < .0001) versus untreated patients (Figure 6F). Figure 6G shows the significantly increased level of 8-OHdG in patients with smoking status (smokers vs non-smokers; p < .01). Non-significant increase in 8-OHdG level was observed in the case of patients with different age groups (<52 years vs ≥52 years; p < .19) and gender groups (males vs females; p = .20), as shown in Figure 6G.

The POD and 8-Oxoguanine level diagnostic efficacy was evaluated using ROC curve analysis. Figure 6D and H show the AUC (1.00) for both *POD* and 8-OHdG with sensitivity: 100 and specificity: 100 (p < .0001).

Discussion

Exosomes as messengers carry cargo that can promote cancer development, progression, and metastasis. Exosomes may facilitate promoting pre-metastatic niche, angiogenesis, and evading the immune system. Exosomal unique cargo material reflects the physiological/pathological state of the donor cell and may serve as potential biomarkers.[23,24] These characteristics suggest analyzing circulating exosomes and their cargo as promising

candidates for cancer liquid biopsy, disease biomarker discovery, monitoring disease progression, and potentially estimating prognosis. miR-17-92 plays major roles in multiple biological processes like proliferation, apoptosis, metabolism, tumorigenesis, and metastasis.[25] However, despite the deregulation of miR-17-92 has been observed in various cancers,[25,26] but involvement of miR-17-92 as the exosomal cargo in HNC carcinogenesis remains unexplored. Among the miR-17-92 cluster, expression deregulation of exosomal miR-19a and miR-19b and their related genes (SMAD2 and SMAD4) has already been reported in our previous study.[20] The involvement of a remaining member of the exosomal miR-17-92 cluster, exosomal miR-17 and exosomal miR-20a, and their targeted gene *TGFBR2* in HNC has not been reported previously. The present study was conducted in three phases. In the first phase, exosomes were isolated from HNC patients and control samples. The isolated exosomes were then characterized based on size distribution and quantification, morphology, and surface markers.

During the characterization of isolated exosomes, NTA was used to calculate the size and concentration of exosomes. The NTA results showed the isolated exosomes had a mean size of 100 nm which is within an estimated size range of exosomes (40-150 nm). The morphology of exosomes was confirmed sphere-shaped using TEM-negative staining, within the anticipated size range of exosomes. These results are in accordance with previous NTA results and this typical form has already been reported in previous findings.[27] Exosomes were immuno-labelled with CD-63 specific marker (commonly used marker

for exosomes) and TEM showed positive labeling. ELISA was used to confirm *CD9*, *CD63,* and *CD81* positive protein surface markers of exosomes in accordance with previous study.[28] Tetraspanin family members including CD9, CD63, and CD81 have been identified as reliable markers for exosome detection and play key roles in the regulation of several functional and molecular processes in cancer.[29]

In the second phase of the present study, the expressional analysis of exosomal miRNAs (miR-17 and miR-20a) and their targeted genes *TGFBR2* was analyzed in 400 HNC patients and 400 controls. The expression of exosomal miRNAs and target genes was correlated with demographic and clinicopathological parameters of HNC patients. Dysregulation of miRNAs is involved in carcinogenesis including HNC cancer.[26] Exosomal miRNAs are considered preferable biomarkers to the other extracellular miRNAs. In the current study, we found significant downregulation of miR-17 in serum exosomes of HNC patients compared to controls, and significantly reduced expressions were observed in advanced stages of HNC patients. The miR-17 has also been associated with several cancers and performs key functions in the regulation of biological properties in cancer cells.[25,26] Consistent with our results downregulation of miR-17 has also been found in breast cancer serum exosomes.[11] The downregulation of miR-17 has also been reported in various cancers like prostate cancer[30] and stomach cancer.[31] miR-17 downregulation has also been reported in therapy-resistant cases of lung cancer.[32] miR-17-92 cluster has been found deleted in various cancers like 21.9% in breast cancer, 20% in melanomas, and 16.5% in ovarian cancer, and functions as a cancer suppressor.[33]

In this study, significant downregulation of miR-20a was found in serum exosomes of HNC patients versus controls, while this downregulation was found pronounced in aggressive-stage HNC patients compared to early-stage patients. Consistent with our results, the cancer suppressor role of miR-20a has been observed in small cell lung cancer,[34] endometrial cancer,[35] breast cancer,[36] and glioma patients.[37] The reason behind the downregulation of miR-20a and miR-17 in our study needs to be further explored. However, one possibility of this downregulation is increased oxidative stress levels in the exosomes of HNC patients. This increased oxidative stress ultimately results in increased necrosis, invasion, metastasis, and aggressiveness of disease. The second possible reason is the interaction of selected miRNAs with hypoxia-inducible factor-1 alpha subunit (HIF-1 α) which participates in the progression and pathogenesis of many cancers.[38,39] HIF-1α plays a role in angiogenesis, cancer development, metastasis, and hypoxic microenvironment.[40] He et al have reported that the deregulation of HIF-1α downregulates miR-20a and miR-17 by reducing the expression of c-Myc and increasing carcinogenesis in AML.[17]

In the present study, exosomal *TGFBR2* was found significantly upregulated in HNC patients versus controls and this upregulation was observed more pronounced in the advanced stages of HNC. Consistent with our findings, the downregulation of miR-17 enhances migration and proliferation of gastric cancer by negatively regulating *TGFBR2* expression.[41] Galunisertib, a *TGFBR2* inhibitor, significantly increases the overall survival of pancreatic cancer patients and serves as a potential drug.[42] In non-squamous cell lung cancer, downregulation of the miR-17 and miR-20a/b led to metastasis and drug resistance by increasing *TGFBR2* expression.[43] Yang et al have revealed that miR-20a binds to the 3′-UTR of *TGFBR2* and inhibits the anti-cancer role of TGF-β in NSCLC.[44]

We found non-significant upregulation of miR-17, miR-20a and target gene *TGFBR2* in treated patients (which were receiving any form of therapeutic strategy including surgery, chemotherapy and radiation) as compared to those patients which were newly diagnosed and were not getting any therapeutic strategy yet. Interestingly, Jank et al have reported increased staining of *TGFBR1*, one of the key members of TGF-β pathway and suggested as a prognostic marker for HNSCC. Jank et al also evaluated inhibition of *TGFBR1* inhibitor using vactosertib and found radio-sensitizing and antineoplastic effects in vitro.[45]

Oxidative stress biomarkers are associated with the pathogenesis of HNC and could be utilized for timely diagnosis. Based on the key pathogenic role of oxidative stress in HNC, several oxidative stress markers have been identified to have promising diagnostic value.[46] In third part of study, oxidative stress was also measured in the exosomes of HNC patients, and its diagnostic value was assessed. The oxidative stress level was correlated with expression levels of selected microRNAs and target gene. The levels of oxidative stress were assessed by measuring antioxidant enzyme peroxidase (POD) and 8-hydroxy-2-deoxyguanosine (*8-OHdG*) levels in isolated exosomes of HNC patients and controls. The POD levels were significantly reduced in HNC patients compared to controls, especially in advanced clinical stages of HNC patients. The *8-OHdG* levels were significantly increased in HNC patients and advanced clinical stages of HNC patients. Oxidative stress, characterized by elevated levels of reactive oxygen species (ROS), has been associated with various pathologies including cancer development, progression, and drug resistance.[47] The increased levels of ROS can cause oxidative damage to DNA, lipids, and proteins through 8-OHdG. Thus, maintaining ROS homeostasis is crucial for preventing oxidative damage and cells utilize antioxidant molecules like POD to achieve this balance.[48] In the present study the association of increased *8-OHdG* levels, increased reactive oxygen species (ROS) and decreased antioxidant enzymes may lead to increased DNA oxidation and ultimately toward aggressiveness of head and neck cancer.[49,50] However, there is no published study available investigating the role of exosomal *8-OHdG* and POD levels leading towards aggressiveness of HNC patients. These results provide valuable insights into the role of oxidative markers in exosomes and highlight their potential as biomarkers for HNC progression and aggressiveness.

Certain limitations to our study exist, such as: first, detailed in-vitro and in-vivo exosome-based studies are required to understand the mechanism through which the deregulation of these molecules leads to HNC pathogenesis. Second, further study with a larger cohort is suggested to understand the therapeutic potential of exosomal miR-17, miR-20a, and *TGFBR2* in HNC. Inflammation is an important contributing factor in HNC.

Carcinogens and mutagens are present in tobacco smoke leading to chronic inflammation which ultimately results in cancer of the head and neck region.[51] Third, to determine the role of inflammation in HNC, certain inflammatory markers need to be assessed in future studies. The level of inflammatory markers will be correlated with the level of selected microRNAs/genes to illuminate the picture of head and neck carcinogenesis.

Conclusion

In the current study, we observed significant downregulation of miR-17, miR-20a, and upregulation of important TGF-β pathway member, *TGFBR2* in serum exosomes of HNC patients than controls. This dysregulation was associated with increased oxidative stress (measured by *8-OHdG* and antioxidant enzyme) and aggressiveness of disease pathology. Further analysis revealed the good diagnostic and poor prognostic significance of selected exosomal microRNAs and *TGFBR2* in HNC patients. The present study suggested that deregulation of miR-17, miR-20a, and *TGFBR2* along with oxidative stress could enhance the diagnostic and prognostic ability and may act as potential/promising and noninvasive biomarkers for HNC patients. Based on our findings, *TGFBR2* is a potential candidate as therapeutic target against HNC, and future studies may evaluate the potential of increased exosomal miR-17/20a or inhibitor of *TGFBR2* as a therapeutic target against HNC.

Author Contributions Statements

All of the authors read and approved the final version of the manuscript. Muhammad Rizwan and Muhammad Shahbaz Haris collected and isolated the exosomes from HNC and control samples. Muhammad Rizwan and Muhammad Shahbaz Haris performed the expression analysis experiments. Muhammad Rizwan, Muhammad Shahbaz Haris, and Fouzia Qayyum performed oxidative stress measurement experiments. Ishrat Mahjabeen and Muhammad Rizwan performed statistical analyses of the data and draft of the manuscript. Mahmood Akhtar Kayani and Ishrat Mahjabeen supervised the project and provided critical revisions. All the authors discussed the results and commented on the manuscript.

Declaration of Conflicting Interests

The authors declared no potential conflicts of interest with respect to the research, authorship, and/or publication of this article.

Ethics Statement

The authors state that they have obtained the appropriate institutional review board approval committee of COMSATS University Islamabad's (CUI) Biosciences department, and cooperating hospitals approval number (CUI/Bio/ERB/4-21/1) or have followed the principles outlined in the Declaration of Helsinki for all human or animal experimental investigations. In addition, for investigations involving human subjects, informed consent has been obtained from the participants involved.

Data Availability

The data supporting the findings of this study are not publicly available due to privacy and ethical restrictions. Protecting the privacy of study participants is a priority, and therefore, the data cannot be shared openly.

ORCID iDs

Muhammad Rizwan [ID] https://orcid.org/0000-0002-0903-0957
Ishrat Mahjabeen [ID] https://orcid.org/0000-0002-6392-672X
Mahmood Akhtar Kayani [ID] https://orcid.org/0000-0001-9886-180X

Supplemental Material

Supplemental material for this article is available online.

References

1. Attar E, Dey S, Hablas A, et al. Head and neck cancer in a developing country: A population-based perspective across 8 years. *Oral Oncol.* 2010;46(8):591–596.

2. Bray F, Ferlay J, Soerjomataram I, Siegel RL, Torre LA, Jemal A. Global cancer statistics 2018: GLOBOCAN estimates of incidence and mortality worldwide for 36 cancers in 185 countries. *CA Cancer J Clin.* 2018;68(6):394–424.

3. Sung H, Ferlay J, Siegel RL, et al. Global cancer statistics 2020: GLOBOCAN estimates of incidence and mortality worldwide for 36 cancers in 185 countries. *CA Cancer J Clin.* 2021;71(3):209–249.

4. Johnson DE, Burtness B, Leemans CR, Lui VWY, Bauman JE, Grandis JR. Head and neck squamous cell carcinoma. *Nat Rev Dis Primers.* 2020;6(1):92.

5. Sala M, Ros M, Saltel F. A complex and evolutive character: Two face aspects of ECM in tumor progression. *Front Oncol.* 2020;10(28):1620.

6. Denaro N, Merlano MC, Russi EG. Follow-up in head and neck cancer: Do more does it mean do better? A systematic review and our proposal based on our experience. *Clin Exp Otorhinolaryngol.* 2016;9(4):287–297.

7. Kalluri R, LeBleu VS. The biology, function, and biomedical applications of exosomes. *Science.* 2020;367(6478):eaau6977.

8. Ruivo CF, Adem B, Silva M, Melo SA. The biology of cancer exosomes: Insights and new perspectives. *Cancer Res.* 2017;77(23):6480–6488.

9. Maas SL, Breakefield XO, Weaver AM. Extracellular vesicles: Unique intercellular delivery vehicles. *Trends Cell Biol.* 2017;27(3):172–188.

10. Jiang X, Hu S, Liu Q, Qian C, Liu Z, Luo D. Exosomal microRNA remodels the tumor microenvironment. *PeerJ.* 2017;22(5):e4196.

11. Lv S, Wang Y, Xu W, Dong X. Serum exosomal miR-17-5p as a promising biomarker diagnostic biomarker for breast cancer. *Clin Lab*. 2020;66(9):p1823.

12. Zhang Y, Zhang Y, Yin Y, Li S. Detection of circulating exosomal miR-17-5p serves as a novel non-invasive diagnostic marker for non-small cell lung cancer patients. *Pathol Res Pract*. 2019;215(8):152466.

13. Langevin S, Kuhnell D, Parry T, et al. Comprehensive microRNA-sequencing of exosomes derived from head and neck carcinoma cells in vitro reveals common secretion profiles and potential utility as salivary biomarkers. *Oncotarget*. 2017;8(47):82459–82474.

14. Zhang X, Li Y, Qi P, Ma Z. Biology of MiR-17-92 cluster and its progress in lung cancer. *Int J Med Sci*. 2018;15(13):1443–1448.

15. Cuzziol CI, Marzochi LL, Possebon VS, et al. Regulation of VEGFA, KRAS, and NFE2L2 oncogenes by MicroRNAs in head and neck cancer. *Int J Mol Sci*. 2022;23(13):7483.

16. Hui AB, Lin A, Xu W, et al. Potentially prognostic miRNAs in HPV-associated oropharyngeal carcinoma. *Clin Cancer Res*. 2013;19(8):2154–2162.

17. He M, Wang Q, Yin Q, et al. HIF-1α downregulates miR-17/20a directly targeting p21 and STAT3: A role in myeloid leukemic cell differentiation. *Cell Death Differ*. 2013;20(3):408–418.

18. Lv X, Wang L, Zhu T. MiR-20a-5p suppressed TGF-β1-triggered apoptosis of human bronchial epithelial BEAS-2B cells by targeting STAT3. *Mol Cell Probes*. 2020;50(1):101499.

19. Sivadas VP, George NA, Kattoor J, Kannan S. Novel mutations and expression alterations in SMAD3/TGFBR2 genes in oral carcinoma correlate with poor prognosis. *Genes, Chromosomes Cancer*. 2013;52(11):1042–1052.

20. Rizwan M, Mahjabeen I, Ashraf NS, Arshad M, Haris MS, Kayani MA. Dysregulation of exosomal miRNAs and their related genes in head and neck cancer patients. *Future Oncol*. 2024;20(21):1–15.

21. Livak KJ, Schmittgen TD. Analysis of relative gene expression data using real-time quantitative PCR and the $2^{-\Delta\Delta CT}$ method. *methods*. 2001;25(4):402–408.

22. Hussain MZ, Haris MS, Rizwan M, Ashraf NS, Arshad M, Mahjabeen I. Deregulation of exosomal miRNAs in rheumatoid arthritis patients. *Plos one*. 2023;18(7):e0289301.

23. Hoshino A, Costa-Silva B, Shen T-L, et al. Tumour exosome integrins determine organotropic metastasis. *Nature*. 2015;527(7578):329–335.

24. Nimir M, Ma Y, Jeffreys SA, et al. Detection of AR-V7 in liquid biopsies of castrate resistant prostate cancer patients: A comparison of AR-V7 analysis in circulating tumor cells, circulating tumor RNA and exosomes. *Cells*. 2019;8(7):688.

25. Zhao W, Gupta A, Krawczyk J, Gupta S. The miR-17-92 cluster: Yin and Yang in human cancers. *Cancer Treat Res Commun*. 2022;33(1):100647.

26. Mestdagh P, Boström A-K, Impens F, et al. The miR-17-92 microRNA cluster regulates multiple components of the TGF-β pathway in neuroblastoma. *Mol Cell*. 2010;40(5):762–773.

27. Jung MK, Mun JY. Sample preparation and imaging of exosomes by transmission electron microscopy. *JoVE J Vis Exp*. 2018(131):e56482.

28. Zlotogorski-Hurvitz A, Dayan D, Chaushu G, Salo T, Vered M. Morphological and molecular features of oral fluid-derived exosomes: Oral cancer patients versus healthy individuals. *J Cancer Res Clin Oncol*. 2016;142(1):101–110.

29. Ashraf NS, Mahjabeen I, Hussain MZ, et al. Role of exosomal miRNA-19a/19b and PTEN in brain tumor diagnosis. *Future Oncol*. 2023;19(22):1563–1576.

30. Ottman R, Levy J, Grizzle WE, Chakrabarti R. The other face of miR-17-92a cluster, exhibiting tumor suppressor effects in prostate cancer. *Oncotarget*. 2016;7(45):73739–73753.

31. Zeng Q, Jin C, Chen W, et al. Downregulation of serum miR-17 and miR-106b levels in gastric cancer and benign gastric diseases. *Chin J Cancer Res*. 2014;26(6):711.

32. Chatterjee A, Chattopadhyay D, Chakrabarti G. miR-17-5p down-regulation contributes to paclitaxel resistance of lung cancer cells through altering beclin1 expression. *PLoS ONE*. 2014;9(4):e95716.

33. Zhang L, Huang J, Yang N, et al. microRNAs exhibit high frequency genomic alterations in human cancer. *Proc Natl Acad Sci USA*. 2006;103(24):9136–9141.

34. Miao Y, Li J, Qiu X, Li Y, Wang Z, Luan Y. miR-27a regulates the self renewal of the H446 small cell lung cancer cell line in vitro. *Oncol Rep*. 2013;29(1):161–168.

35. He Y, Ma H, Wang J, Kang Y, Xue Q. Mir-20a-5p inhibits endometrial cancer progression by targeting janus kinase 1. *Oncol Lett*. 2021;21(5):1–7. doi:10.3892/ol.2021.12688

36. Yu Z, Willmarth NE, Zhou J, et al. microRNA 17/20 inhibits cellular invasion and tumor metastasis in breast cancer by heterotypic signaling. *Proc Natl Acad Sci USA*. 2010;107(18):8231–8236.

37. Yang B, Meng Q, Sun Y, Gao L, Yang J. Long non-coding RNA SNHG16 contributes to glioma malignancy by competitively binding miR-20a-5p with E2F1. *J Biol Regul Homeost Agents*. 2018;32(2):251–261.

38. Semenza GL. Targeting HIF-1 for cancer therapy. *Nat Rev Cancer*. 2003;3(10):721–732.

39. Nicholas SA, Sumbayev VV. The involvement of hypoxia-inducible factor 1 alpha in toll-like receptor 7/8-mediated inflammatory response. *Cell Res*. 2009;19(8):973–983.

40. Hanahan D, Weinberg RA. Hallmarks of cancer: The next generation. *cell*. 2011;144(5):646–674.

41. Qu Y, Zhang H, Duan J, et al. MiR-17-5p regulates cell proliferation and migration by targeting transforming growth factor-β receptor 2 in gastric cancer. *Oncotarget*. 2016;7(22):33286–33296.

42. Melisi D, Garcia-Carbonero R, Macarulla T, et al. Galunisertib plus gemcitabine vs. Gemcitabine for first-line treatment of patients with unresectable pancreatic cancer. *Br J Cancer*. 2018;119(10):1208–1214.

43. Jiang Z, Yin J, Fu W, et al. MiRNA 17 family regulates cisplatin-resistant and metastasis by targeting TGFbetaR2 in NSCLC. *PLoS ONE*. 2014;9(4):e94639.

44. Yang S, Cho Y-J, Jin L, et al. An epigenetic auto-feedback loop regulates TGF-β type II receptor expression and function in NSCLC. *Oncotarget*. 2015;6(32):33237–33252.

45. Jank BJ, Schnoell J, Kladnik K, et al. Targeting TGF beta receptor 1 in head and neck squamous cell carcinoma. *Oral Dis*. 2024;30(3):1114–1127.

46. Singh A, Pandey P, Tewari M, Pandey H, Gambhir I, Shukla H. Free radicals hasten head and neck cancer risk: A study of total

oxidant, total antioxidant, DNA damage, and histological grade. *J Postgrad Med.* 2016;62(2):96–101.

47. Chio IIC, Tuveson DA. ROS In cancer: The burning question. *Trends Mol Med.* 2017;23(5):411–429.

48. Xu Z, Zhang L, Pan M, et al. A bionanozyme with ultrahigh activity enables spatiotemporally controlled reactive oxygen species generation for cancer therapy. *Adv Funct Mater.* 2021;31(40): 2104100.

49. Kumar A, Pant MC, Singh HS, Khandelwal S. Assessment of the redox profile and oxidative DNA damage (8-OHdG) in squamous cell carcinoma of head and neck. *J Cancer Res Ther.* 2012;8(2):254–259. doi:10.4103/0973-1482.98980

50. Nandakumar A, Nataraj P, James A, Krishnan R, Mahesh K. Estimation of salivary 8-hydroxydeoxyguanosine (8-OHdG) as a potential biomarker in assessing progression towards malignancy: A case-control study. *Asian Pac J Cancer Prev APJCP.* 2020;21(8):2325–2329.

51. Agnihotri R, Gaur S. Implications of tobacco smoking on the oral health of older adults. *Geriatr Gerontol Int.* 2014;14(3): 526–540.